Conical Third-Harmonic Generation in Normally Dispersive Media

Virgilijus Vaičaitis,* Vygandas Jarutis, and Dionysios Pentaris†
Laser Research Center, Vilnius University, Sauletekio 10, Vilnius LT-10223, Lithuania
(Received 15 February 2009; published 2 September 2009)

It is shown, both theoretically and experimentally, that in normally dispersive media under tight-focusing conditions third harmonic is generated by six-wave mixing rather than via common third-order frequency tripling. Though far-field pattern of third-harmonic signal was an axially symmetric ring for a wide range of the material wave vector mismatch and laser beam focusing conditions, in some cases the generation of more complex beams has been found possible. Results of simulations of the proposed model qualitatively correspond well with experimental data for the calculated values of third- and fifth-order nonlinear susceptibilities of sodium.

DOI: 10.1103/PhysRevLett.103.103901 PACS numbers: 42.65.Ky, 42.65.An, 42.65.Re

Third-harmonic generation (THG) in gases using third-order nonlinearity is an important source of coherent UV and vacuum ultraviolet (VUV) radiation. Usually, in order to increase the efficiency of THG focused laser beams are used. Unfortunately, in isotropic normally dispersive materials light generated prior to the focus destructively interferes with that generated beyond the focus and the total THG efficiency becomes negligible under the tight-focusing condition [1]. Thus, the tunability of such light sources is limited to comparably narrow spectral regions of negative material dispersion. However, for sufficiently intense incident optical fields the higher-order polarizations can be comparable to or larger than the lower-order ones. Therefore, THG is also possible through six-wave mixing, which is feasible both for normally and negatively dispersive media. Moreover, the tight focusing of the pump beam should increase the signal of the six-wave mixing and reduce the efficiency of the common THG in normally dispersive media (Fig. 1). However, though the far-field intensity distribution of radiation generated by this process in normally dispersive media was believed to be a circularly symmetric ring pattern [2,3], no experimental evidence has been provided to support this theoretical prediction. Note that various conical structures have been extensively studied previously in liquids and gases in order to elucidate the nature of so-called conical emission (see, for example, [4–6] and references therein), supercontinuum generation [7] as well as generation of conical or X waves [8,9].

Though ring-shaped third-harmonic patterns were registered in a number of experiments with air [9–12], argon [13], and some other gases [14], conical THG has never been interpreted as the result of six-wave mixing. On the other hand, there were many reports of unusual dependence of the third-harmonic generation efficiency on the intensity of incident beam [15–18], but this phenomenon has been explained mainly as a consequence of nonlinear phase shifts of interacting fields induced by the optical Kerr effect. Only in a few papers [3,19] laser frequency tripling was explained as being induced by a six-wave mixing rather than by third-order process, but conical THG has not been observed during these experiments. However, for example, in helium the ratio of fifth- and third-order nonlinear susceptibilities $\chi^{(5)}/\chi^{(3)}$ is approximately 10^{-10} cm^3/erg [20] and fifth-order polarization becomes comparable to the third-order one for the laser intensity of $I = 5 \times 10^{12}$ W/cm^2. Such laser intensity levels were used in a number of experiments with gases. Assuming the same or even lower ratio of $\chi^{(5)}/\chi^{(3)}$ for atmospheric air and noble gases ($\chi^{(5)} \sim 10^{-29} - 10^{-28}$ esu for argon and xenon [21,22]) one may expect at least non-negligible contribution to THG from six-wave mixing under the typical conditions of filamented Ti:sapphire laser pulses (typical filamentary structures of beam waist diameter $2w \sim 100$ μm, 1 mJ energy and peak intensities of

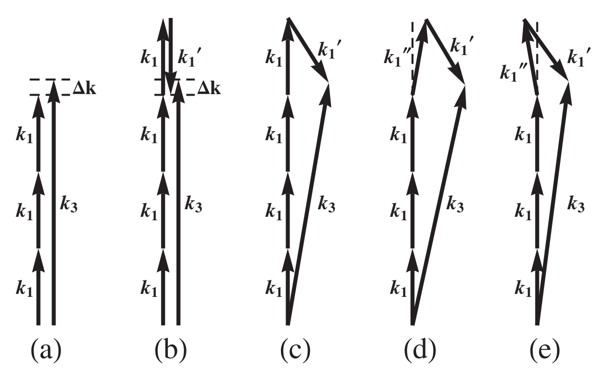

FIG. 1. Wave vector diagrams illustrating common THG (a) and six-wave mixing (b)–(e) in normally dispersive media for the collinear (a),(b) and focused (c)–(e) pump. In the collinear case both processes are not phase matched and thus inefficient. The pump beam focusing further increases phase mismatch $\mathbf{\Delta k}$ for the common THG but allows the noncollinear phase matching of six-wave mixing (c)–(e). Since the intensity of the off-axis light of the focused Gaussian beam is always lower than that on-axis only the most efficient cases of conical six-wave mixing with a few off-axis wave vectors involved are shown (c)–(e).

10^{13}–10^{14} W/cm^2) [23,24]. Therefore, even at moderate pump intensities six-wave mixing should be taken into account as a source of laser frequency tripling or at least as a seed for the four-wave processes producing conical and/or highly divergent THG which has been registered in a number of experiments with air and other gases exposed to intense femtosecond laser pulses [9–13,18].

In this Letter we present the results of both the theoretical analysis and experiment demonstrating conical THG in normally dispersive medium (sodium vapor). We have shown that in such media third-harmonic is generated mainly by six-wave mixing for a wide range of material wave vector mismatch and laser beam focusing conditions. In addition, we have demonstrated that, though far-field pattern of such THG signal is mainly an axially symmetric ring, in some cases generation of more complex third-harmonic beams is possible.

For the theoretical description of THG we used the same notation as in [25], i.e., the real electric field amplitude $\mathcal{E}(\omega)$ is given by the following expression: $\mathcal{E}(\omega) = \tilde{E}(\omega) \times \exp(-i\omega t) + \text{c.c.} = A(\omega)\exp(ikz - i\omega t) + \text{c.c.}$ The third- and fifth-order polarizations $P^{(3)}$ and $P^{(5)}$ (source of THG) are given by (here and further $\omega_3 = 3\omega_1$)

$$P^{(3)}(\omega_3) = \varepsilon_0 D^{(3)} \chi^{(3)} \tilde{E}^3(\omega_1), \tag{1}$$

$$P^{(5)}(\omega_3) = \varepsilon_0 D^{(5)} \chi^{(5)} \tilde{E}^4(\omega_1) \tilde{E}^*(\omega_1), \tag{2}$$

where $D^{(3)} = 1$ and $D^{(5)} = 5$ are degeneracy factors of the considered fields. Assuming third-harmonic generation being a week process, a wave propagation equation for the slowly varying third-harmonic (TH) pulse complex field envelope A_3 under the nondepleted pump approximation is given by

$$\frac{\partial A_3}{\partial z} - \frac{i}{2k_3}\Delta_\perp A_3 - \frac{1}{u_3}\frac{\partial A_3}{\partial t} = i(\sigma^{(3)} + \sigma^{(5)}|A_1|^2) A_1^3 e^{i\Delta k z}, \tag{3}$$

where the subscripts 1 and 3 denote the fundamental and TH pulses, respectively, and $\Delta k = 3k_1 - k_3$ is phase mismatch. The nonlinear coefficients $\sigma^{(j)}$ ($j = 3, 5$) are linked to the third- and fifth-order nonlinear optical susceptibilities $\chi^{(3)}$ and $\chi^{(5)}$ by the relations

$$\sigma^{(3)} = \frac{k_3}{2n_3^2} D^{(3)} \chi^{(3)}(-\omega_3; \omega_1, \omega_1, \omega_1), \tag{4}$$

$$\sigma^{(5)} = \frac{k_3}{2n_3^2} D^{(5)} \chi^{(5)}(-\omega_3; \omega_1, \omega_1, \omega_1, \omega_1, -\omega_1). \tag{5}$$

We also assume that the spatial profile of incident pulse is TEM_{00} Gaussian mode optimally focused into a positively dispersive medium at $z = 0$, i.e.,

$$A_1 = \frac{A_{10}}{s} \exp\left[-\frac{1}{s}\left(\frac{r}{w}\right)^2 - \frac{1}{\tau^2}\left(t - \frac{z}{u_1}\right)^2\right], \tag{6}$$

where $s = 1 + iz/L_d$ with w and $L_d = k_1 w^2/2$ being the radius of the pump beam waist and Rayleigh length, respectively. $k_1 = \omega_1 n_1/c$ represents the wave number, where n_1 is the refraction index of the medium, while τ and u_1 denote the pulse width and its group velocity. It is worthwhile to note that the theoretical model does not take into account higher-order dispersion effects such as group velocity dispersion, as well as other types of nonlinear interactions such as self-modulation of the pump pulse. It was found that all of these effects have an indistinguishable influence under the conditions of our experiment.

The experimentally observed far-field intensity distribution of TH radiation is proportional to $\int |S_3|^2 dt$, where S_3 is a spatial Fourier transform of A_3. As this intensity distribution possesses circular symmetry it is convenient to represent it in terms of its angular spectrum. Denoting angle $\theta = k_\perp/k_3 = \sqrt{k_x^2 + k_y^2}/k_3$ one can show that the far-field intensity distribution of TH is proportional to dimensionless function

$$\mathcal{S}(\theta) = \frac{1}{\tau}\int_{-\infty}^{\infty} |M_3(\theta, t) + \gamma M_5(\theta, t)|^2 dt, \tag{7}$$

where $\gamma = \sigma^{(5)} A_{10}^2/\sigma^{(3)}$, and $M_{3,5}$ are dimensionless functions determined from the equation $\sigma^{(3)} M_3 + \sigma^{(5)} M_5 = |S_3|/(L_d \pi w^2 A_{10}^3)$. It follows from Eq. (7) that when $\gamma < 1$ third-harmonic radiation is generated mainly by the $\chi^{(3)}$ process, while for $\gamma > 1$ the $\chi^{(5)}$ process quickly becomes dominant. In Fig. 2 the dependencies of normalized $\int |M_5(\theta, t)|^2 dt$ on the propagation angle for various values of the pump beam waist radius w and mismatch Δk are presented. One can see that in many cases the far-field intensity distribution of generated radiation is a ring pattern, symmetric to the optical axis of the laser beam [Fig. 2(a) curves 3,4; Fig. 2(b) curve 2]. However, for a wide range of w and Δk ($\Delta k < 0$) TH beam structure is different: it may consist of a single axial component or of a mixture of axial and conical parts [Fig. 2(a) curves 1,2, and Fig. 2(b) curves 1,3,4]. In addition, when the pump focusing is not so tight and $\gamma < 1$, the impact of third-order nonlinear polarization becomes non-negligible, causing generation of conical TH beam with a lower intensity ratio between its axial and conical parts. It is interesting to note that a conical TH beam component can be present even when $\Delta k = 0$, i.e., when phase-matching conditions are fully satisfied [see Fig. 2(b), curve 1]. This result, however, is related with group velocity dispersion and valid only for the case of short pump pulses.

To test the results of these calculations, we have performed a proof-of-principle experiment of third-harmonic generation in sodium vapor excited by femtosecond laser pulses. As a light source an optical parametric generator (OPG) pumped by a femtosecond Ti:sapphire laser (central wavelength 800 nm, pulse duration 120 fs (FWHM), pulse energy 0.5 mJ) has been used. Single-pulse energy of IR femtosecond pulses produced by the OPG was 4–6 μJ. The beam having the diameter $2w_0$ of about 10 mm

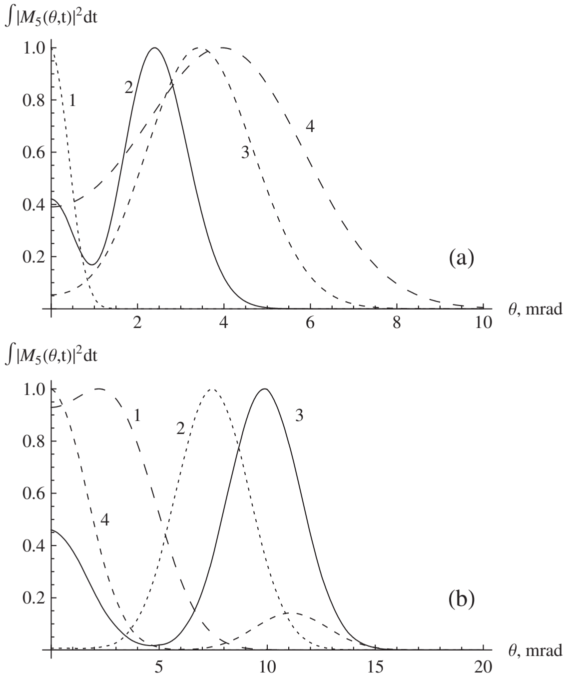

FIG. 2. Dependence of $\int_{-\infty}^{\infty} |M_5(\theta, t)|^2 dt$ on θ for various focusing and mismatching conditions: (a) $\Delta k = -0.4\ \mathrm{cm}^{-1}$ and (1) $w = 630\ \mu\mathrm{m}$, (2) $w = 210\ \mu\mathrm{m}$, (3) $w = 130\ \mu\mathrm{m}$, (4) $w = 90\ \mu\mathrm{m}$; (b) $w = 90\ \mu\mathrm{m}$ and (1) $\Delta k = 0\ \mathrm{cm}^{-1}$, (2) $\Delta k = -3\ \mathrm{cm}^{-1}$, (3) $\Delta k = -7\ \mathrm{cm}^{-1}$, (4) $\Delta k = -9\ \mathrm{cm}^{-1}$.

(FWHM) was focused into the center of the sodium cell using lenses of various focal lengths. The length of the heated section of the cell was 15–20 cm and its temperature was monitored with thermocouples. The pressure of the Ar buffer gas was about 10 Torr at room temperature of the heated section.

Conical THG has been observed for sodium vapor densities ranging from 5×10^{13} to $2 \times 10^{16}\ \mathrm{cm}^{-3}$ and for the pump wavelength tuned between 1770 and 2200 nm. In this spectral region $\Delta k < 0$ since sodium vapor is normally dispersive medium for the wavelengths longer than 589.5 nm. The typical experimentally obtained far-field third-harmonic pattern is presented in Fig. 3 (inset). The cone angle of third-harmonic emission increased with the power of the pump focusing lens [see Fig. 4(a)] and/or sodium vapor density. The distinct feature of this conical radiation is the large angular spread ($\Delta\theta/\theta_0 > 1$, Fig. 3), which well corresponds to the theoretical predictions and is typical for the difference frequency mixing in isotropic media [26,27].

The nonlinear optical susceptibilities of sodium were calculated based on quantum-mechanical perturbation theory of the atomic wave function using values of the dipole matrix elements of lowest 12 energy levels [28]. Thus for the pump wavelength $\lambda_1 = 1.98\ \mu\mathrm{m}$ and sodium vapor density $N = 3 \times 10^{15}\ \mathrm{cm}^{-3}$ we have estimated that $\chi^{(3)} \sim 2.5 \times 10^{-26}\ (\mathrm{m/V})^2$ (or 1.8×10^{-18} esu), and $\chi^{(5)} \sim 2.1 \times 10^{-45}\ (\mathrm{m/V})^4$ (or 1.4×10^{-28} esu). The amplitude

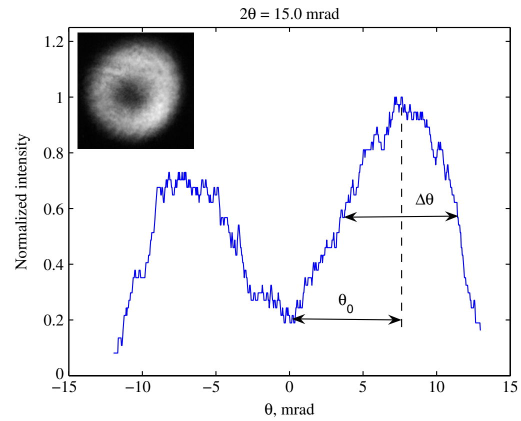

FIG. 3 (color online). Typical far-field pattern (inset) and angular spectrum of conical TH for the pump wavelength of 1980 nm and sodium vapor density of $3 \times 10^{15}\ \mathrm{cm}^{-3}$. The power of focusing lens was 2 diopters.

of the pump beam given by Eq. (6) is determined by expression $A_{10}^2 = (2/\pi)^{1/2}(\varepsilon_0 c n_1)^{-1} E_1/(\pi w^2 \tau)$, where E_1 is the fundamental pulse energy. Under typical conditions of experiment ($E_1 = 4$–$7\ \mu\mathrm{J}$, $\tau = 140$ fs, $w = 60\ \mu\mathrm{m}$) one estimate that the ratio $\gamma = \sigma^{(5)} A_{10}^2/\sigma^3 \sim 1$.

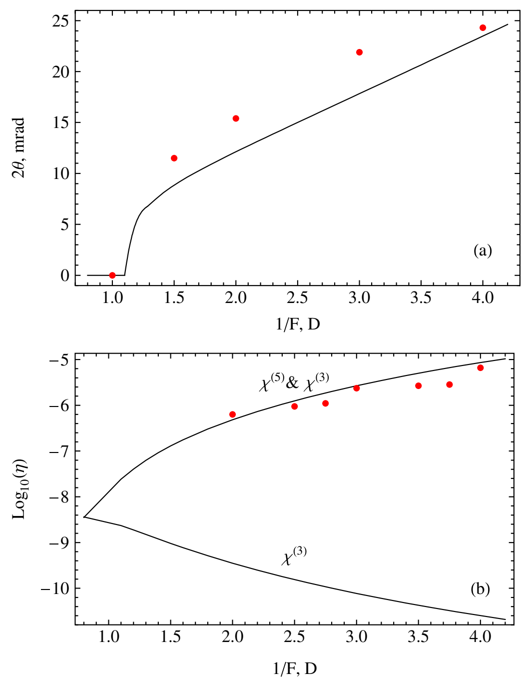

FIG. 4 (color online). Dependencies of third-harmonic cone angle 2θ (a) and generation efficiency η (b) on the power of focusing lens $1/F$ for sodium vapor density of $3 \times 10^{15}\ \mathrm{cm}^{-3}$. The pump wavelength was 1980 nm (a) and 1900 nm (b). The points are experimentally obtained data, solid lines represent the results of theoretical calculations, obtained for $E_1 = 4\ \mu\mathrm{J}$, $\tau = 140$ fs, $w_0 = 5$ mm, and length of nonlinear medium $L = 10$ cm. Line denoted by $\chi^{(3)}$ and $\chi^{(5)}$ presents the total efficiency of THG, while the relative contribution of the cubic nonlinearity is denoted as $\chi^{(3)}$.

This means that the impact of the $\chi^{(5)}$ process into TH generation is indeed of the same order as that of the $\chi^{(3)}$ process. However, as it was mentioned above, the efficiency of frequency tripling through third-order nonlinearity is negligibly small under tight-focusing conditions, while there is no such limitation for six-wave mixing. Moreover, even when the process of six-wave mixing is phase mismatched for collinear interacting waves, the vectorial phase matching still can be satisfied since the focused fundamental beam contains some angular spread of its components.

Third-harmonic conversion efficiency η can be represented as

$$\eta = \frac{E_3}{E_1} = \left(\frac{2}{\pi}\right)^{1/2} (k_3 L_d w A_{10}^2 \sigma^{(3)})^2 \int_0^\infty \mathcal{S}(\theta)\theta d\theta. \quad (8)$$

As it follows from this expression, η sharply increases as beam waist radius w decreases $[w = F\lambda/(w_0 \pi n)]$, in agreement with the experimental results (Fig. 4). Some discrepancies at large focusing lens powers can be explained by the influence of higher-order optical nonlinearities on the self-focusing of pump pulses [24], which has not been taken into account in our model. It is worthwhile to note that the contribution of $\chi^{(3)}$ nonlinearity to the total TH conversion efficiency sharply decreases with the pump focusing lens power, in agreement with the theory [1].

Note that the conical third-harmonic generation in normally dispersive media is also possible through the use of seventh-order nonlinearity, when six pump photons are annihilated to create two third-harmonic photons [29]. However, this process is genuinely parametric [30], and therefore is far less efficient than the six-wave mixing proposed in this Letter. Indeed, for the parametric process $A_3^{(\mathrm{param})} \sim \chi^{(7)} A_1^6 A_3^*$, while for the six-wave mixing $A_3^{(\mathrm{mix})} \sim \chi^{(5)} A_1^4 A_1^*$. Thus, even assuming that $\chi^{(7)} A_1^4 \sim \chi^{(5)} A_1^2$ one obtains

$$\left|\frac{A_3^{(\mathrm{param})}}{A_3^{(\mathrm{mix})}}\right| = \left|\frac{(\chi^{(5)} A_1^2) A_1^2 A_3^*}{\chi^{(5)} A_1^4 A_1^*}\right| = \left|\frac{A_3^*}{A_1^*}\right| \ll 1 \quad (9)$$

according to our experimental data [see Fig. 4(b)].

In conclusion, we have shown, both theoretically and experimentally, that in normally dispersive media under tight-focusing conditions of femtosecond laser pulses the dominant mechanism of THG can be the process of six-wave mixing. To the best of our knowledge, conical TH has been generated and explained as a result of six-wave mixing for the first time. Though conical THG has been demonstrated in a simple atomic system, obtained results indicate that this phenomenon can also take place in other normally dispersive media, such as air and noble gases. In addition, we have shown that in some cases apart from conical THG produced by six-wave mixing generation of more complex TH beams is possible.

The authors wish to acknowledge support from LASERLAB-EUROPE CONT-European Laser Laboratories Integrated Initiative Continued (Contract No. 212025) and from a Marie Curie Early Stage Training project ATLAS funded through the European Commission's Framework Programme 6 (FP6, Contract No. MEST-CT-2004-8048).

*virgilijus.vaicaitis@ff.vu.lt
†Permanent address: Laser, Non linear and Quantum Optics Labs, Physics Department, University of Patras, Patras, Greece 26500.

[1] R. W. Boyd, *Nonlinear Optics* (Academic Press, San Diego, CA, 2003), 2nd ed., p. 114.
[2] A. Lago, G. Hilber, and R. Wallenstein, Phys. Rev. A **36**, 3827 (1987).
[3] J. Kutzner and H. Zacharias, Appl. Phys. B **66**, 571 (1998).
[4] B. D. Paul, M. L. Dowell, A. Gallagher, and J. Cooper, Phys. Rev. A **59**, 4784 (1999).
[5] V. Vaicaitis and E. Gaizauskas, Phys. Rev. A **75**, 033808 (2007).
[6] H. Skenderovic *et al.*, Phys. Rev. A **77**, 063816 (2008).
[7] F. Theberge *et al.*, Opt. Lett. **33**, 2515 (2008).
[8] M. Kolesik, E. M. Wright, and J. V. Moloney, Phys. Rev. Lett. **92**, 253901 (2004).
[9] H. Xiong *et al.*, Phys. Rev. A **77**, 043802 (2008).
[10] N. Akozbek *et al.*, Phys. Rev. Lett. **89**, 143901 (2002).
[11] F. Theberge *et al.*, Opt. Commun. **276**, 298 (2007).
[12] H. X. Xu *et al.*, Appl. Phys. Lett. **92**, 011111 (2008).
[13] J. Peatross *et al.*, J. Opt. Soc. Am. B **15**, 186 (1998).
[14] S. Y. Chen, A. Maksimchuk, E. Esarey, and D. Umstadter, Phys. Rev. Lett. **84**, 5528 (2000).
[15] M. S. Malcuit, R. W. Boyd, W. V. Davis, and K. Rzazewski, Phys. Rev. A **41**, 3822 (1990).
[16] R. A. Ganeev *et al.*, Appl. Phys. B **41**, 69 (1986).
[17] G. Marcus, A. Zinger, and Z. Henis, J. Opt. Soc. Am. B **16**, 792 (1999).
[18] R. A. Ganeev *et al.*, Appl. Opt. **45**, 748 (2006).
[19] R. A. Ganeev *et al.*, Opt. Commun. **184**, 305 (2000).
[20] J. Reintjes, C.-Y Che, and R. C. Eckardt, IEEE J. Quantum Electron. **14**, 581 (1978).
[21] A. L. 'Huillier *et al.*, in *Atoms in Intense Laser Fields*, edited by M. Gavrila (Academic Press, San Diego, CA, 1992), pp. 139–201.
[22] N. L. Manakov and V. D. Ovsyannikov, Zh. Eksp. Teor. Fiz. **52**, 895 (1980) [Sov. Phys. JETP **79**, 1769 (1980)].
[23] S. Tzortzakis *et al.*, Phys. Rev. Lett. **86**, 5470 (2001).
[24] A. Vincotte and L. Berge, Phys. Rev. A **70**, 061802(R) (2004).
[25] R. L. Sutherland, *Handbook of Nonlinear Optics* (Marcel Dekker, Inc., New York, 1996), 2nd ed., p. 13–14.
[26] G. Bjorklund, IEEE J. Quantum Electron. **11**, 287 (1975).
[27] V. Vaicaitis, Opt. Commun. **185**, 197 (2000).
[28] R. B. Miles and S. E. Harris, IEEE J. Quantum Electron. **9**, 470 (1973).
[29] K. D. Moll, D. Homoelle, A. L. Gaeta, and R. W. Boyd, Phys. Rev. Lett. **88**, 153901 (2002).
[30] S. Meyer, B. N. Chichkov, and B. Wellegehausen, J. Opt. Soc. Am. B **16**, 1587 (1999).